HTML ABSTRACT + LINKS

Properties of nonpolar *a*-plane InGaN/GaN multiple quantum wells grown on lateral epitaxially overgrown *a*-plane GaN

Arpan Chakraborty, Stacia Keller, Cedrik Meier, Benjamin A. Haskell,[a] Salka Keller, Patrick Waltereit, Steven P. DenBaars,[a] Shuji Nakamura,[a] James S. Speck,[a] and Umesh K. Mishra[a),b)]
ECE and Materials Departments, University of California–Santa Barbara, Santa Barbara, California 93106

(Received 9 September 2004; accepted 29 November 2004; published online 7 January 2005)

The properties of nonpolar *a*-plane InGaN/GaN multiple-quantum wells (MQWs), grown simultaneously on lateral epitaxially overgrown (LEO) *a*-plane GaN and planar *a*-plane GaN, were studied. High-resolution x-ray diffraction analysis revealed that the In mol fraction in the MQWs grown on LEO-GaN was significantly lower than that on planar *a*-plane GaN. The lower In incorporation was confirmed by microphotoluminescence (μ-PL) and wide-area photoluminescence measurements, which showed a redshift of the MQW emission from 413 nm for the nearly defect-free laterally overgrown regions to 453 nm for the defective "window" regions of the LEO *a*-plane GaN, to 478 nm for the high-defect density planar *a*-plane GaN. μ-PL measurements also demonstrated that the emission from the nearly defect-free wings of the LEO *a*-plane GaN was more than ten times stronger than the emission from the defective windows. © *2005 American Institute of Physics*. [DOI: 10.1063/1.1851007]

Current state-of-the-art III-nitride-based optoelectronic devices employing heterostructures grown along the polar *c* direction are characterized by the presence of polarization-induced electrostatic fields. The internal electric fields result in the spatial separation of the electron and hole wave functions within quantum wells and give rise to the quantum confined Stark effect.[1,2] The corresponding reduction in oscillator strength and redshift of optical transitions limits the performance of the optoelectronic devices, especially in the green and ultraviolet regions of the spectrum. One promising means of eliminating internal field effects in the nitrides is through the growth of wurtzite device structures with nonpolar orientations, e.g., growth along the *m* and *a* directions. In recent years, various groups including ours have confirmed the absence of polarization effects in nonpolar III-nitride-based heterostructures.[3–6] More recently, we demonstrated nonpolar *a*-plane InGaN/GaN light-emitting diode (LED) exhibiting a drive-current independent electroluminescence peak indicating the absence of polarization-induced electric field in the quantum wells.[7]

Growth of high quality nonpolar InGaN/GaN quantum wells is required for the realization of visible and near-ultraviolet nonpolar nitride-based LEDs and laser diodes. In comparison to *c*-plane InGaN/GaN multiple-quantum wells (MQWs),[8] very little is known about the structural and optical properties of nonpolar InGaN/GaN MQWs grown on *a*-plane GaN. This is primarily because of the poor structural properties of planar *a*-plane GaN grown on *r*-plane sapphire and *a*-plane SiC substrates.[9,10] However, by applying the lateral epitaxial overgrowth (LEO) technique,[11,12] the limitation of obtaining heterostructures and devices of superior structural quality along nonpolar directions has been overcome.[7,13,14] In this letter, we report on the properties of nonpolar $(11\bar{2}0)$ *a*-plane InGaN/GaN MQWs grown by metalorganic chemical vapor deposition (MOCVD) on both reduced-defect density LEO *a*-plane GaN and high-defect density planar *a*-plane GaN. The In incorporation, surface morphology, and photoluminescence characteristics of the MQWs on the low extended defect-density wing regions of the laterally overgrown region were compared to the properties of the MQWs grown on the defective window regions as well as on the high-defect density planar *a*-plane GaN template.

The InGaN/GaN MQW samples studied here were regrown simultaneously on both 10-μm-thick, fully coalesced, reduced-dislocation density *a*-plane LEO GaN templates fabricated by hydride vapor phase epitaxy (HVPE) and on MOCVD grown 2-μm-thick planar *a*-plane GaN templates. For comparison a 2-μm-thick planar *c*-plane GaN template was also co-loaded during the regrowths. Details of the HVPE-based LEO GaN template process may be found elsewhere.[12] The mask for this particular LEO template consisted of parallel 15-μm-wide SiO_2 stripes separated by 5-μm-wide window openings oriented parallel to the GaN $\langle 1\bar{1}00\rangle$ direction. Transmission electron microscopy (TEM) on similar samples[12] revealed that the threading dislocation (TD) and basal plane stacking fault (SF) densities in the overgrown GaN were below $\sim 5\times 10^6\ \mathrm{cm}^{-2}$ and $3\times 10^3\ \mathrm{cm}^{-1}$, respectively. The TD and SF densities in the window region of the LEO GaN template were $\sim 9\times 10^9\ \mathrm{cm}^{-2}$ and $4\times 10^5\ \mathrm{cm}^{-1}$, respectively. Previously conducted TEM investigations on planar *a*-plane GaN template showed TD and SF densities on the order of $\sim 2.6\times 10^{10}\ \mathrm{cm}^{-2}$ and $3.8\times 10^5\ \mathrm{cm}^{-1}$, respectively.[9] The InGaN/GaN MQW structures were grown in a vertical close-spaced showerhead MOCVD reactor using TMGa, TMIn, DiSi, and NH_3 (supplied by Showa Denko KK.) as precursors. First a 1-μm-thick Si-doped GaN layer was deposited on the templates, followed by 12 periods of InGaN/GaN MQWs with Si-doped GaN barriers. Following the growth, symmetric high-resolution x-ray diffraction (HRXRD) ω–2θ scans were

[a]Also at: ERATO JST, UCSB Group, Santa Barbara, California 93106.
[b]Electronic mail: mishra@ece.ucsb.edu

 © 2005 American Institute of Physics
Downloaded 10 Jan 2005 to 134.91.46.22. Redistribution subject to AIP license or copyright, see http://apl.aip.org/apl/copyright.jsp

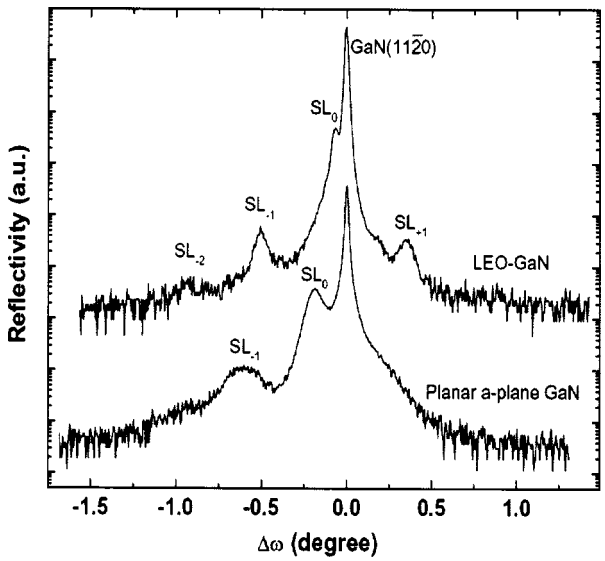

FIG. 1. HRXRD ω–2θ scans for the InGaN/GaN MQWs grown in the same growth run on (a) LEO *a*-plane GaN, and (b) planar *a*-plane GaN template.

recorded with a Philips MRD X'Pert PRO triple axis diffractometer to determine the structural parameters of the MQWs. Atomic force microscopy (AFM) performed on a Digital Instruments D3000 operating in tapping mode was used to image the surface morphology. The optical characterization was carried out at room temperature using an UV-microphotoluminescence (μ-PL) system in confocal geometry. A reflecting microscope objective (52×, n.a. 0.65) was used to excite the sample and collect the signal at the same time. For excitation, the 325 nm line of a He–Cd laser (cw, 17 mW) was used. The final spot diameter was ~3 μm. The μ-PL signal was analyzed using a 0.55 m spectrometer and a CCD camera. Wide-area cw PL measurements were carried out using the 325 nm line of a He–Cd laser with an excitation power density of ~20 W/cm^2.

Figure 1 shows a comparison of the ω–2θ scans for concurrently grown InGaN/GaN MQWs on LEO *a*-plane GaN and planar *a*-plane GaN template, revealing a significant difference in the In composition between the LEO and the planar *a*-plane film. The structural parameters of the quantum wells were obtained by analyzing the angular positions of the satellite peaks, and based on the growth times of the wells and the barriers. For the MQWs grown on the LEO template, the average In composition in the wells was determined to be 4.4% with the well and barrier thicknesses being 27 and 87 Å, respectively. For the MQWs grown on the planar *a*-plane GaN, the average In composition of the wells was 12.5%, and the well and barrier thicknesses were 30 and 90 Å, respectively. The In composition in the MQWs grown on the *c*-plane GaN sample was so high that the sample had yellow color and reliable structural parameters could not be extracted from the x-ray scan.

Figure 2 shows a 20 μm × 20 μm AFM micrograph of the surface of the InGaN/GaN MQWs (terminated by an InGaN well) grown on a LEO *a*-plane GaN template. Smooth and rough areas were clearly visible in the micrograph. The virtually defect-free Ga-face wings, growing along the [0001] direction, exhibited a smooth surface morphology with minimal surface pitting. On the N-face wings, growing along the [000$\bar{1}$] direction, however, surface defects (pits) formed leading to an increase in surface roughness.

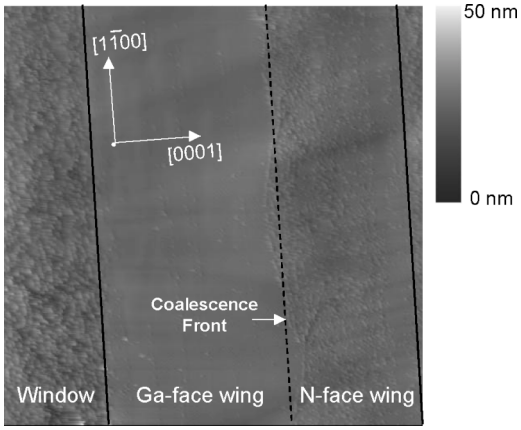

FIG. 2. 20 μm × 20 μm AFM micrograph showing the surface morphology in the Ga-face wing, N-face wing, and the window regions of the LEO sample (grayscale = 50 nm).

The highest density of surface pits was observed in the dislocated window region, resulting in an extremely rough surface morphology. The observation of surface defects is closely related to the presence of microstructural defects in the material.[12]

Figure 3 shows a contour plot of the μ-PL measurement performed on the MQWs grown on the LEO GaN template. The scan direction was perpendicular to the stripe direction (i.e., along [0001]). Two adjacent stripes were spatially scanned at intervals of 1 μm. At every position, the PL emission intensity was plotted for the spectral range $340 < \lambda < 500$ nm. Strong quantum well emission around 410 nm was observed from the reduced-dislocation density wings. In contrast, the emission from the defective window regions was an order of magnitude lower in intensity. Also, a second emission peak around 450 nm was observed from the windows. Figure 4(a) compares the PL spectra taken from regions on the Ga-face wing, the N-face wing, and the window of the LEO sample. Whereas only one strong emission peak, at 413 nm with a full width at half maximum of 22.7 nm, was seen on the Ga-face wing; two emission peaks, at 413 and 446 nm, were recorded on the N-face wing. Both peaks were about half as intense as the emission from the nearly

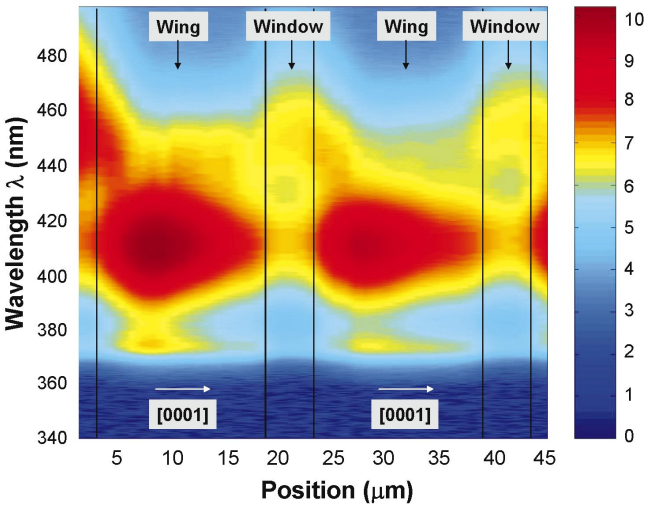

FIG. 3. (Color) Contour plot of the μ-PL intensity on the wing and window regions of the LEO sample as a function of the wavelength (the intensity is plotted in a logarithmic scale).

Downloaded 10 Jan 2005 to 134.91.46.22. Redistribution subject to AIP license or copyright, see http://apl.aip.org/apl/copyright.jsp

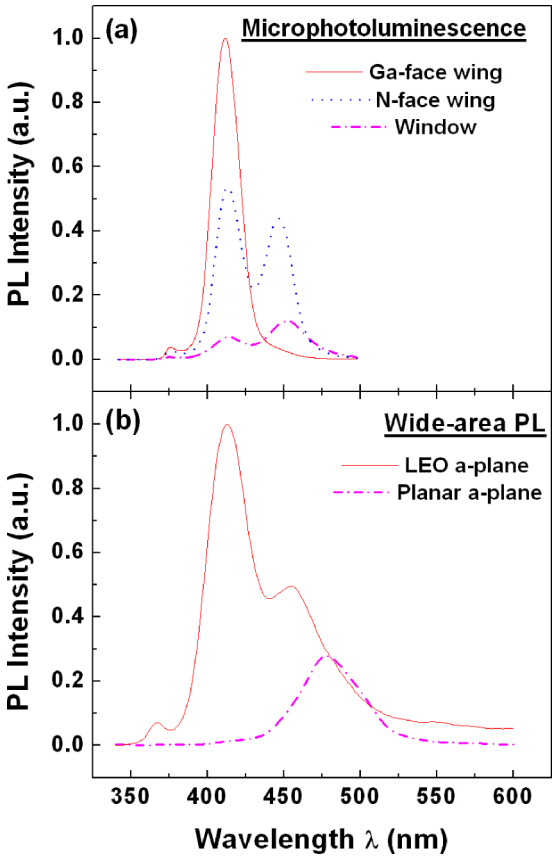

FIG. 4. (Color online) (a) μ-PL measurements on the Ga-face wing, N-face wing, and the window region of the LEO sample; (b) Wide-area PL measurement on the LEO sample and the planar *a*-plane sample.

defect-free Ga-face wing. Two weak emission peaks at ~410 and 453 nm were recorded from the defective windows as well. The appearance of the longer wavelength emission peaks in the N-face and window regions were correlated with the surface defects observed by AFM.

Wide-area PL measurements were performed on the same LEO sample as was examined with μ-PL [Fig. 4(b)]. The spectra were characterized by a strong emission peak at 413 nm and the presence of a broad shoulder at ~450 nm. As revealed in the μ-PL measurements, the shoulder can be attributed to the emission from the N-face wing and the window regions of the LEO sample. In contrast, wide-area PL measurement on the planar *a*-plane InGaN/GaN MQW sample exhibited only one peak at 478 nm with about one-fourth less intense emission compared to that from the LEO sample. The lower PL intensity and the absence of a shorter wavelength emission peak from the planar sample are the result of the significantly higher defect-density in the relatively thin *a*-plane GaN template.

The longer wavelength PL emission from the planar *a*-plane sample agreed with the higher In content, determined from the HRXRD analysis. The results showed that the In incorporation and hence the PL emission wavelength was considerably higher in defective material. The presence of surface defects with facets other than the $(11\bar{2}0)$ orientation led to the increased In incorporation in the defective areas. Similar behavior was observed in the presence of the so-called "V-defects" in *c*-plane InGaN/GaN MQWs by Wu *et al.*[15] However the reasons for lower In incorporation efficiency in *a*-plane GaN compared to *c*-plane GaN are unclear. Investigations are in progress to explain the reduced In-incorporation in *a*-plane MQWs and the results will be discussed in a forthcoming paper.

In conclusion, nonpolar *a*-plane InGaN/GaN MQWs were grown on reduced-defect density LEO GaN templates as well as on high-defect density planar *a*-plane GaN templates. μ-PL measurements of the MQWs grown on the LEO GaN template showed a ten times stronger emission in the reduced-defect density wing compared to that from the defective window region. The μ-PL measurements also revealed the presence of an additional longer wavelength emission peak in the defective regions of the LEO sample. Evidence for enhanced indium incorporation in quantum wells grown on defective planar *a*-plane GaN in comparison to reduced defect density LEO *a*-plane GaN was also seen in wide area PL and HRXRD measurements. The enhanced indium incorporation was linked to the presence of surface-defects on the sample.

The authors would like to acknowledge the partial support of the Solid State Lighting and Display Center at UCSB. This work made use of the MRL Central Facilities supported by the MRSEC Program of the National Science Foundation under Award No. DMR00-80034. Fabrication of the HVPE-grown LEO templates used in this work was supported by the NICP/JST Exploratory Research for Advanced Technology Program. C.M. acknowledges the support of Deutsche Forschungsgemeinschaft Grant No. ME 2087-1.

[1] T. Takeuchi, S. Sota, M. Katsuragawa, M. Komori, H. Takeuchi, H. Amano, and I. Akasaki, Jpn. J. Appl. Phys., Part 2 **36**, L382 (1997).
[2] F. Bernardini, V. Fiorentini, and D. Vanderbilt, Phys. Rev. B **56**, R10024 (1997).
[3] P. Waltereit, O. Brandt, A. Trampert, H. T. Grahn, J. Menniger, M. Ramsteiner, M. Reiche, and K. H. Ploog, Nature (London) **406**, 865 (2000).
[4] H. M. Ng, Appl. Phys. Lett. **80**, 4369 (2002).
[5] M. D. Craven, P. Waltereit, F. Wu, J. S. Speck, and S. P. DenBaars, Jpn. J. Appl. Phys., Part 2 **42**, L235 (2003).
[6] Y. J. Sun, O. Brandt, S. Cronenberg, S. Dhar, H. T. Grahn, K. H. Ploog, P. Waltereit, and J. S. Speck, Phys. Rev. B **67**, 041306 (2003).
[7] A. Chakraborty, B. A. Haskell, S. Keller, J. S. Speck, S. P. DenBaars, S. Nakamura, and U. K. Mishra, Appl. Phys. Lett. **85**, 5143 (2004).
[8] S. Nakamura and G. Fasol, *The Blue Laser Diode* (Springer, Heidelberg, 1997).
[9] M. D. Craven, S. H. Lim, F. Wu, J. S. Speck, and S. P. DenBaars, Appl. Phys. Lett. **81**, 469 (2002).
[10] M. D. Craven, F. Wu, A. Chakraborty, B. Imer, U. K. Mishra, S. P. DenBaars, and J. S. Speck, Appl. Phys. Lett. **84**, 1281 (2004).
[11] M. D. Craven, S. H. Lim, F. Wu, J. S. Speck, and S. P. DenBaars, Appl. Phys. Lett. **81**, 1201 (2002).
[12] B. A. Haskell, F. Wu, M. D. Craven, S. Matsuda, P. T. Fini, T. Fujii, K. Fujito, S. P. DenBaars, J. S. Speck, and S. Nakamura, Appl. Phys. Lett. **83**, 644 (2003).
[13] T. Koida, S. F. Chichibu, T. Sota, M. D. Craven, B. A. Haskell, J. S. Speck, S. P. DenBaars, and S. Nakamura, Appl. Phys. Lett. **84**, 3768 (2004).
[14] C. Chen, M. Shatalov, E. Kuokstis, V. Adivarahan, M. Gaevski, S. Rai, and M. A. Khan, Jpn. J. Appl. Phys., Part 2, Part 2 **43**, L1099 (2004).
[15] X. H. Wu, C. R. Elsass, A. Abare, M. Mack, S. Keller, P. M. Petroff, S. P. DenBaars, J. S. Speck, and S. J. Rosner, Appl. Phys. Lett. **72**, 692 (1998).

Downloaded 10 Jan 2005 to 134.91.46.22. Redistribution subject to AIP license or copyright, see http://apl.aip.org/apl/copyright.jsp